

# Shoot-Silicon-Signal protein to regulate root silicon uptake in rice

Received: 11 July 2024

Accepted: 8 December 2024

Published online: 27 December 2024

 Check for updatesNaoki Yamaji<sup>1,5</sup>✉, Namiki Mitani-Ueno<sup>1,5</sup>, Toshiki Fujii<sup>1</sup>, Tomonori Shinya<sup>1</sup>, Ji Feng Shao<sup>2</sup>, Shota Watanuki<sup>3</sup>, Yasunori Saitoh<sup>3,4</sup> & Jian Feng Ma<sup>1</sup>

Plants accumulate silicon to protect them from biotic and abiotic stresses. Especially in rice (*Oryza sativa*), a typical Si-accumulator, tremendous Si accumulation is indispensable for healthy growth and productivity. Here, we report a shoot-expressed signaling protein, Shoot-Silicon-Signal (SSS), an exceptional homolog of the flowering hormone “florigen” differentiated in Poaceae. SSS transcript is only detected in the shoot, whereas the SSS protein is also detected in the root and phloem sap. When Si is supplied from the root, the SSS transcript rapidly decreases, and then the SSS protein disappears. In *sss* mutants, root Si uptake and expression of Si transporters are decreased to a basal level regardless of the Si supply. The grain yield of the mutants is decreased to 1/3 due to insufficient Si accumulation. Thus, SSS is a key phloem-mobile protein for integrating root Si uptake and shoot Si accumulation underlying the terrestrial adaptation strategy of grasses.

Silicon (Si) is a principal component of soil on the Earth, which is marginally but durably dissolved in soil water as silicic acid {Si(OH)<sub>4</sub>} and provided to all plants rooting in the soil. Most land plants can utilize Si as a beneficial element to protect them from various biotic and abiotic stresses<sup>1</sup>. Si is deposited as amorphous silica (SiO<sub>2</sub>) on the surface of the leaves and other aerial organs of plants and mitigates pathogen infection, herbivore eating, nutrient imbalance, water/temperature stresses, lodging, and so on<sup>2</sup>. Not only the physical protection, Si deposition, and/or soluble Si in plants also modulate various stress responses by the plants<sup>3,4</sup>. At least angiosperm (except *Brassicaceae* including *Arabidopsis*, probably) have a pair of Si transporter genes, homologs of silicic acid channel *Lsi1* and silicic acid efflux transporter *Lsi2* in rice<sup>5,6</sup>, for active uptake of Si<sup>7</sup>. Therefore, the acquisition of Si is one of the common strategies of land plants to adapt to the environment on Earth, even though Si is not an essential element for plant life cycles (except for horsetails)<sup>1,2</sup>. Si concentration in the aboveground parts of plants varies largely between species. It is usually higher in graminaceous plants<sup>8</sup>, meaning that the significance of Si utilizing strategy varies in different species. Still, we don't know how it is optimized for the adaptation of each plant. In rice (*Oryza*

*sativa*), a typical Si-accumulating plant, the shoot Si concentration reaches 10% of the dry weight, and mutation of the Si channel gene *Lsi1* results in defect of root Si uptake<sup>5</sup> and serious yield penalty in usual field condition<sup>7,9</sup>. Because of the low solubility of Si(OH)<sub>4</sub> (saturation concentration is about 2 mM at ordinary temperature and pH), active uptake of Si in soils by cereal plants, especially rice, often resulting the depletion of soluble Si in the soil<sup>10,11</sup>. Therefore, Si is recognized as an agronomically essential element, and Si fertilizer is commonly applied for rice production in Japan<sup>11</sup>. Inversely, the knockout of a Si efflux transporter gene *SIET4*, which is a homolog of *Lsi2* and involved in the final step of Si deposition into particular tissues in the leaves, resulted in lethal disorders of stress responses induced by ectopic Si deposition<sup>4</sup>. On the other hand, although Si never shows excess toxicity for any wild-type plants, the expression of *Lsi1* and *Lsi2* in the root are downregulated by continuous Si supply and reduce the root Si uptake ability to the basal level. This down-regulation reflects Si accumulation in the shoot part but is not affected by Si concentration around the root<sup>12</sup>, although the mechanisms for signal transduction from shoot to root were not identified. Thus, rice has systemic regulatory mechanisms to optimize the cost-benefit of Si for better

<sup>1</sup>Institute of Plant Science and Resources, Okayama University, Chuo 2-20-1, Kurashiki 710-0046, Japan. <sup>2</sup>State Key Laboratory of Subtropical Silviculture, Zhejiang Agriculture & Forestry University, Lin'an 311300, China. <sup>3</sup>Graduate School of Environmental, Life, Natural Science and Technology, Okayama University, Tsushima Naka 3-1-1, Kita, Okayama 700-8530, Japan. <sup>4</sup>Research Institute for Interdisciplinary Science, Okayama University, Tsushima Naka 3-1-1, Kita, Okayama 700-8530, Japan. <sup>5</sup>These authors contributed equally: Naoki Yamaji, Namiki Mitani-Ueno. ✉e-mail: [n-yamaji@rib.okayama-u.ac.jp](mailto:n-yamaji@rib.okayama-u.ac.jp)

adaptation on land. Here we report the signaling molecule named Shoot-Silicon-Signal (SSS), which is conserved in graminaceous plants (Supplementary Fig. 1) and is also named FLOWERING LOCUST T-LIKE 12 (OsFTL12) as a homolog of the flowering hormone “florigen” FT<sup>13</sup>. SSS protein is expressed only in the shoot but also reaches the phloem and the root under Si-deficient conditions, and then induces higher expression of transporters for root Si uptake.

## Results

### Identification of Shoot-Silicon-Signal gene

Because we had been focused on the pivotal roles of nodes in the distribution control of mineral nutrients and the organization of the development<sup>14,15</sup>, we conducted transcriptome analysis in rice nodes<sup>16</sup> and found a candidate gene *SSS/OsFTL12* for unidentified signaling process, which has apparently node-specific expression in a field condition (with environmental Si supply) (Fig. 1a). Whereas, during another transcriptome analysis for characterization of Si-hypersensitive phenotype of the *siet4* mutant<sup>4</sup>, *SSS* was also detected in Si-starved leaf blade but almost not in Si-treated leaf blade, which is the most downregulated gene response to the 1 day Si treatment (except very minor express genes)<sup>4</sup>. Thus, we focus on this gene as a potential component of the Si signaling process. *SSS/OsFTL12* gene consists of 5 exons and encodes a protein of 173 amino acid residues with 19.5 kDa deduced molecular weight (Os06g0552900, [https://](https://rapdb.dna.affrc.go.jp)

[rapdb.dna.affrc.go.jp](https://rapdb.dna.affrc.go.jp)), which have 63% identity with both OsHd3a/OsFTL2 and AtFT (major florigen in rice and Arabidopsis, respectively) and belongs to a distinct subgroup only found in graminaceous plants (Supplementary Figs. 1 and 2).

### Gene expression analysis of SSS

Then, we conducted detailed expression analyses of *SSS* by qRT-PCR. At the vegetative growth stage, *SSS* expression was detected in both the shoot basal region containing basal nodes and the other shoot part including leaf blade and leaf sheath in the absence of Si (Fig. 1b). While treated with nutrient solution containing 1 mM silicic acid for 2 days, the expression in both the shoot basal region and the shoot other part were almost disappeared (Fig. 1b). *SSS* transcript was not detected in the root regardless of the Si treatment (Fig. 1b). At the flowering stage, 10-times higher expression of *SSS* was observed in the node I (uppermost node) compared to the flag leaf blade under the without Si condition (Fig. 1c). Continuous Si supply suppressed *SSS* expression in both the node I and flag leaf blade, but basal level expression was remained only in the node (Fig. 1c). That's why *SSS* expression looks nodes specific under field condition (Fig. 1a). When treated with 1 mM Si from the root, *SSS* expression in the vegetative shoot very rapidly responded within a few hours, and reached almost zero after the 16 to 24 h treatment (Fig. 1d). The *SSS* suppression also showed a clear dose-response manner (Fig. 1e). Because orthologs of *SSS/OsFTL12* are

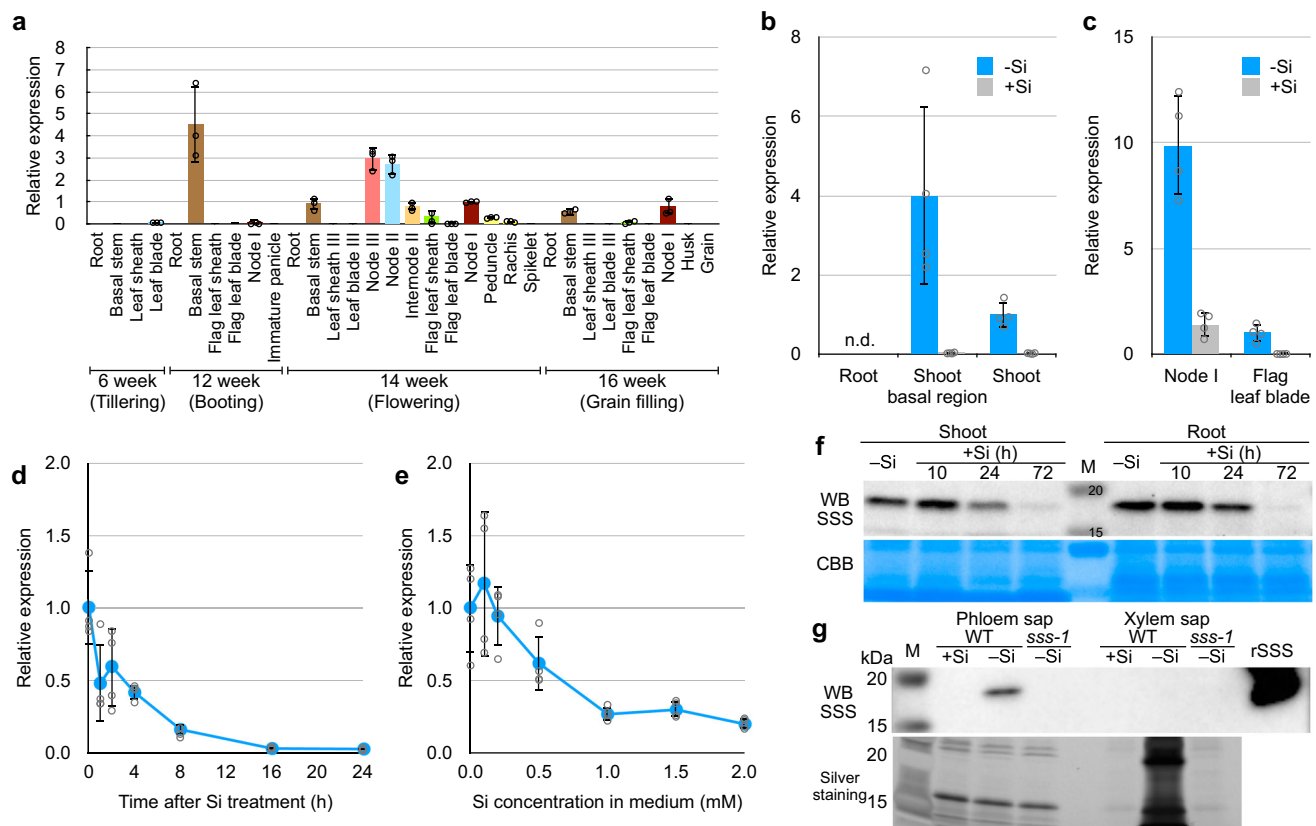


**Fig. 1 | Gene and protein expression of SSS response to Si. a–e** Expression of *SSS* gene determined by qRT-PCR. **a** Expression in paddy field condition in various organs at vegetative and reproductive growth stages of WT rice. **b** Si response at the vegetative stage. WT rice grown hydroponically without Si was treated with or without 1 mM Si for the last 2 days. **c** Si response at the flowering stage. WT rice is grown hydroponically with or without 1 mM Si continuously. **d** Time-course Si response in vegetative shoot. WT rice grown hydroponically without Si was treated with 1 mM Si for up to 24 h. **e** Si dose-response in vegetative shoot. WT rice grown hydroponically without Si were treated with 0, 0.1, 0.2, 0.5, 1.0, 1.5, and 2.0 mM Si for 6 h. Data are means ± SD of 3 (a) or 4 (b–e) biological replicates. n.d.: not

detected. **f, g** Western blot of SSS protein by antibody against SSS. **f** WT rice grown hydroponically without Si was treated with 1 mM Si for up to 72 h, and the whole shoot and root were used for protein extraction. 18 μg total protein was loaded in each lane. CBB staining was shown as the loading control. **g** WT and *sss-1* mutant rice grown hydroponically with or without Si for 3 days were applied for the insect-laser method. Pure phloem sap (0.18–0.32 μL) and xylem sap (0.5 μL) obtained from the same plants, together with recombinant SSS protein (rSSS, 10 ng), were used. M: protein size marker. Silver staining was shown as the loading control. Source data are provided as a Source Data file.

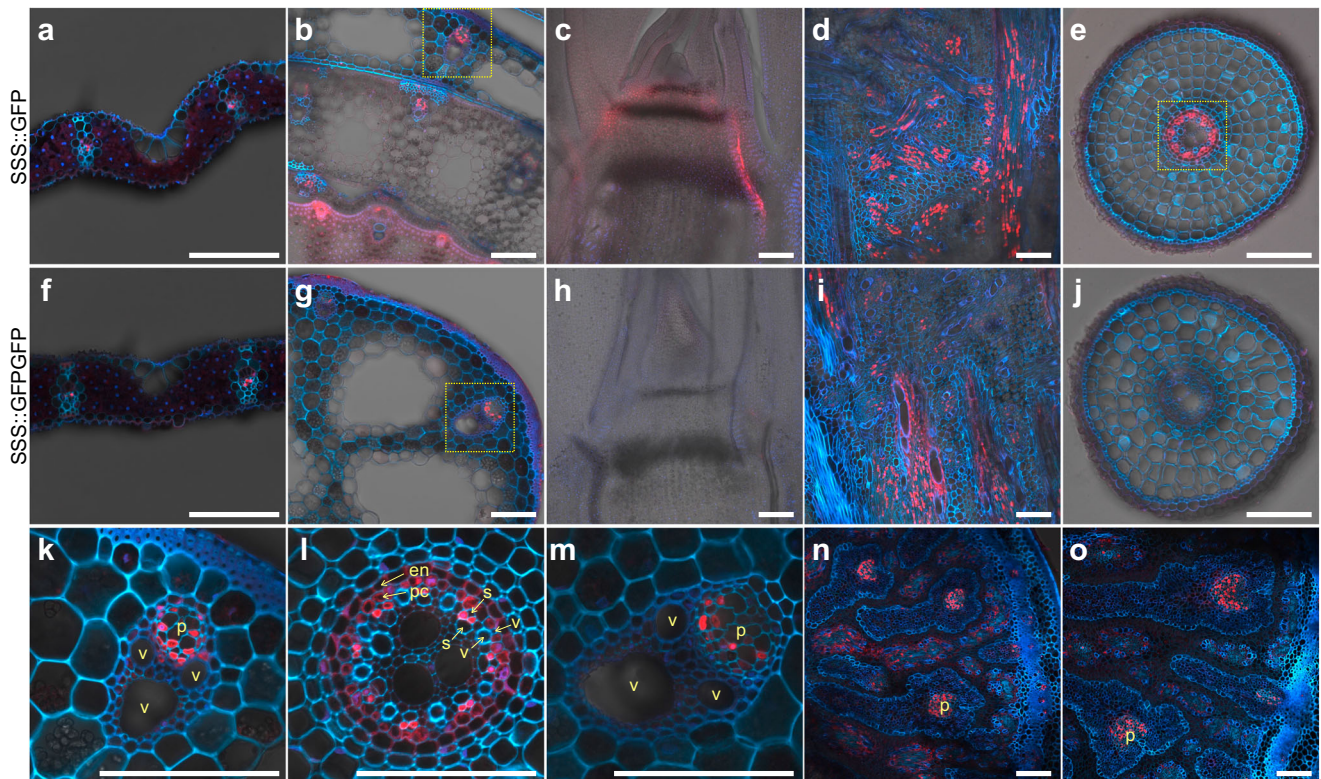


**Fig. 2 | Tissue localization of SSS.** Immunostaining of GFP in transgenic rice carrying pSSS-SSS::GFP (a–e, k, l, n) or pSSS-SSS::GFP::GFP (f–j, m, o) at the vegetative stage grown hydroponically without Si (a–m) or at the flowering stage grown in soil pot (n, o). Cross-section of leaf blade (a, f), leaf sheath (b, g), root (e, j), node I (k, o), and longitudinal-section of shoot apex (c, h) and basal node (d, i) were used.

k–m are magnified images of the yellow dotted box area in (b, e, g), respectively. Red and blue colors indicate signals from secondary antibody and cell wall auto-fluorescence, respectively. p: phloem region, v: xylem vessel, s: sieve tube, pc: pericycle, en: endodermis. Bar = 100  $\mu$ m.

conserved in graminaceous plants (Supplementary Fig. 1), we also checked Si response of these genes in wheat (*Triticum aestivum*), maize (*Zea mays*) and Moso bamboo (*Phyllostachys edulis*). Similar to rice, all these orthologous genes were only expressed in the shoot but not in the root and downregulated by Si treatment (Supplementary Fig. 3), although some differences from rice SSS were observed as below. Wheat has three copies of genes, among them *TaFTL12A* and *D* showed similar expression, but no specific PCR product of *TaFTL12B* was detected (Supplementary Fig. 3a, b). Both *TaFTL12A* and *D* were not expressed in the shoot basal region (including basal nodes) (Supplementary Fig. 3a). Basal level expressions remained in wheat *TaFTL12s* and maize *ZmFTL12* but not in bamboo *PeFTL12* after prolonged Si treatment (Supplementary Fig. 3b, c, d).

### Detection of SSS protein in shoot, root, and phloem sap

In the case of florigen FT/Hd3a, which is mainly expressed in the leaf, the protein moves to shoot apical meristem through the phloem to regulate flowering time<sup>13</sup>. We found that, although the SSS transcript was not detected in the root, the SSS protein was detected in both the shoot and root by western blot analysis using an antibody against SSS (Fig. 1f). The SSS protein signals were gradually diminished till three days Si treatment in both the shoot and root (Fig. 1f), which are much slower than Si response of SSS transcript in the shoot (Fig. 1d), but consistent with the time-course of Si response of *Lsi1*, *Lsi2* expression, and Si uptake in root<sup>12</sup>. Conversely, suppressed SSS protein abundance in the root was recovered by seven days of Si starvation, probably by force of SSS expression in the newly developed leaf during the treatment (Supplementary Fig. 4).

To acquire more direct evidence for the translocation of SSS protein through the phloem, we reinvented the “insect-laser” device, originally invented more than 40 years ago<sup>17</sup>, using a handheld laser

engraver. SSS protein was indeed detected by western blot in obtained phloem sap from the laser-cut stylet of brown planthopper (*Nilaparvata lugens*) sucking Si-deficient rice (Fig. 1g). Neither phloem sap of Si-sufficient rice nor xylem sap with/without Si treatment were contained SSS (Fig. 1g). This result also confirmed by proteome analysis of three independent phloem sap samples (two –Si and one +Si) (Supplementary Table 1), and previous report of rice phloem/xylem proteins<sup>18</sup>.

In addition, we checked Si concentration in phloem and xylem sap. Surprisingly, the phloem sap containing supersaturated Si in both 1 and 0.1 mM silicic acid supplied conditions, although several times more concentrated in the xylem sap (Supplementary Fig. 5).

### Cellular and subcellular localization of SSS protein

To investigate tissue-level localization of SSS protein, we generated transgenic rice carrying a fusion gene between SSS and *Green Fluorescent Protein* (SSS::GFP) or tandem copy of GFP (SSS::GFP::GFP) controlled under SSS promoter. It is expected that due to increased molecular mass, the permeability of SSS::GFP::GFP (73.5 kDa) to plasmodesmata between phloem companion cells and sieve elements, which is essential for phloem loading of proteins<sup>19</sup>, is much lower than that of SSS::GFP (46.5 kDa). Detailed localization of these fusion proteins was revealed by immunohistochemical staining using a GFP antibody. In the leaf blade, leaf sheath, and basal node at the vegetative growth stage, both SSS::GFP and SSS::GFP::GFP were mainly localized phloem parenchyma cells of vascular bundles (Fig. 2). In the root and shoot apex, SSS::GFP localized stele cells and premature vascular tissues (but not reached to the shoot apical meristem different from florigen<sup>13</sup>), respectively, but SSS::GFP::GFP was not detected in these tissues (Fig. 2). Which means that SSS gene (SSS promoter) expressed in phloem in both leaf and nodes but not

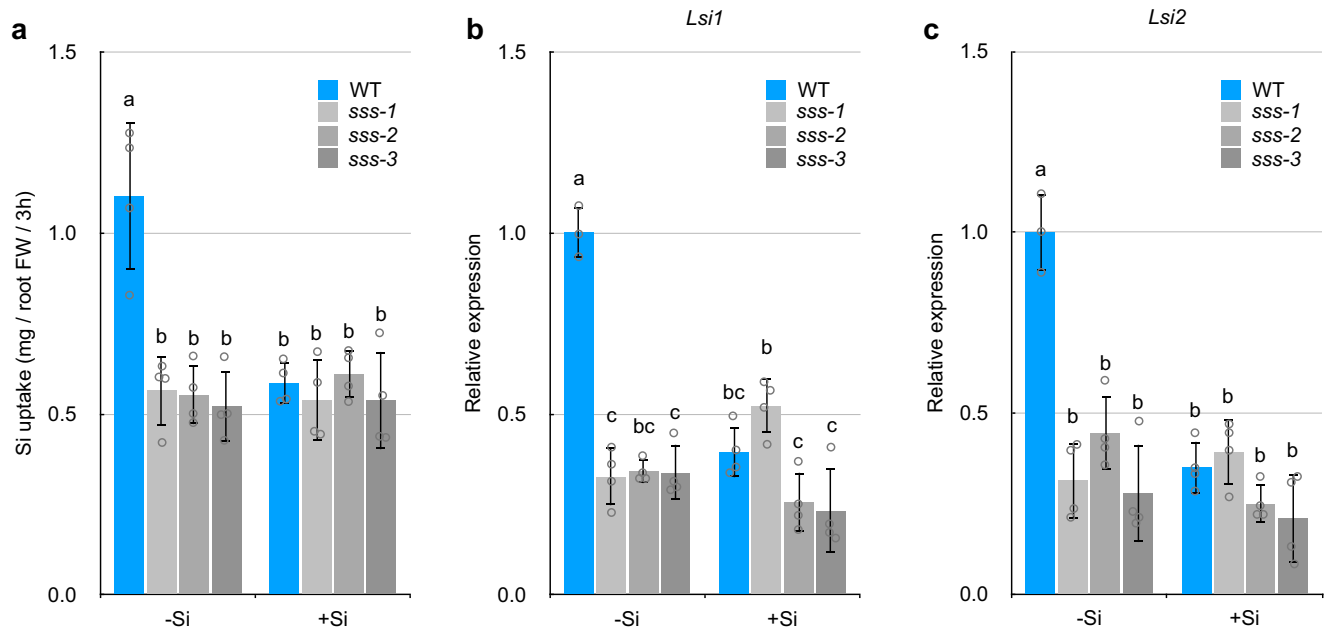


**Fig. 3 | Phenotype of *sss* mutants at the vegetative growth stage.** WT and three independent *sss* knockout mutants cultivated hydroponically without Si for 4 weeks were pre-treated with (+Si) or without (-Si) 1 mM Si for 1 week. Then, each plant was used for **a** 3 h short-term Si uptake experiment, and **b, c** real-time RT-PCR

gene expression analysis of *Lsi1* (**b**) and *Lsi2* (**c**) in the root. Data represent mean  $\pm$  SD of 4 biological replicates. Different letters indicate significant differences with  $p < 0.05$  by two-sided Tukey's test. Source data are provided as a Source Data file.

expressed in the root and shoot apex; SSS::GFP protein translocated from leaves and nodes to the root stele through the phloem, while SSS::GFP:GFP cannot migrate from the originally expressed organs. This mobility of SSS::GFP but not SSS::GFP:GFP protein from the shoot to root is also confirmed by western blot (Supplementary Fig. 6), although the root/shoot SSS::GFP protein ratio is much lower than endogenous SSS protein (Fig. 1f), which might be caused by the side effect of GFP fusion on the protein mobility or/and stability. In more detail, the diffused protein was also observed in parenchyma cells around the phloem of the leaf sheath (Fig. 2k), pericycle and endodermis cells of the root (Fig. 2l) in pSSS-SSS::GFP transgenic line, but not in pSSS-SSS::GFP:GFP line (Fig. 2j, m). In uppermost node I at the flowering stage, these proteins mainly localized the phloem region of the enlarged vascular bundles, which connect to the flag leaf and lower two nodes<sup>15</sup>, and relatively minor signals were also observed in the marginal region of diffuse vascular bundles, which connect to the panicle<sup>15</sup> (Fig. 2n, o).

Subcellular localization of the fusion protein was investigated by double staining of nuclei by DAPI (4', 6-diamidino-2-phenylindole). Signals from SSS::GFP included nuclei signals; therefore, SSS::GFP localized nucleus and cytosol in both the shoot and root (Supplementary Fig. 7). This subcellular localization was also confirmed by transient expression of SSS::GFP or SSS::GFP:GFP in onion epidermal cells (Supplementary Fig. 8).

### Si uptake and Si transporter genes expression in *sss* knockout mutants

To investigate the role of SSS, we prepared three independent knockout mutants of SSS by CRISPER/Cas9 technique at two different target sites at the 1st exon of SSS. The early frame shift mutation results in no protein expression (Fig. 1g and Supplementary Fig. 9). Short-term root Si uptake of the mutants (*sss-1*, -2, and -3) were about half of the wild-type (WT) under Si-deficient condition (Fig. 3a). Pretreatment with 1 mM Si for 1 week resulted in decreased Si uptake to the half of the Si-deficient condition in the WT, while not changed in the mutants, culminate in same level between WT and mutants (Fig. 3a). Similarly, gene expression of two major Si uptake transporters, *Lsi1* and *Lsi2*, was

suppressed to about 1/3 by the Si pretreatment, but the expression in the mutants were retained at basal level as same as the Si sufficient WT regardless of the Si conditions (Fig. 3b, c). This difference in *Lsi1* expression was also confirmed at the protein level by immunostaining of *Lsi1* in the roots (Supplementary Fig. 10).

### Transcriptome analysis of WT and *sss* mutant root response to Si

For comprehensive identification of genes regulated by shoot-derived SSS protein in the root either directly or indirectly, we conducted RNA-seq of WT and *sss-1* root treated with or without 1 mM Si for 2 days (Table S2). When comparing WT -Si and *sss* -Si, 100 genes were downregulated more than 2 times in the *sss* mutant, and most of them (84/100) were also downregulated significantly in WT +Si. Moreover, most of these Si responses (69/84) disappeared in *sss* + Si (Table S2). Among them, three major Si transporter genes, *Lsi1*, *Lsi2*, and *Lsi3*, for root Si uptake and xylem loading<sup>3,6,20</sup> were included. In addition, two known mineral uptake transporters genes, *OsNramp5* for Mn/Cd<sup>21</sup> and *OsMOT1;1* for Mo<sup>22</sup>, were also downregulated by Si (Table S2), the former one is consistent with previous study<sup>23</sup>, although they did not respond to Mn<sup>21</sup>, the latter one is not validated for Si response. Gene ontology (GO) analysis suggested that genes for nicotianamine biosynthesis and light harvesting in photosystem I were enriched, although these physiological meanings are unknown.

On the other hand, 39 genes were upregulated more than twofold in *sss* -Si compared to WT -Si, but these genes are mostly not consistent with Si response in WT (Table S2), and no significant enrichment of GO terms was detected.

### Phenotype of *sss* knockout mutants at the harvest

WT rice and two *sss* mutants were cultured in soil pots, which provide Si continuously. At the harvest, the appearances and height of these plants were not largely different (Fig. 4a, b). Because SSS is a homolog of florigen, we also compared the heading date but almost no difference was observed between WT and the mutants (Fig. 4c). In contrast, panicle number per plant and filled spikelet rate of the mutants were decreased to 51-70% of the WT, and the grain yield was only 26-32% of the WT

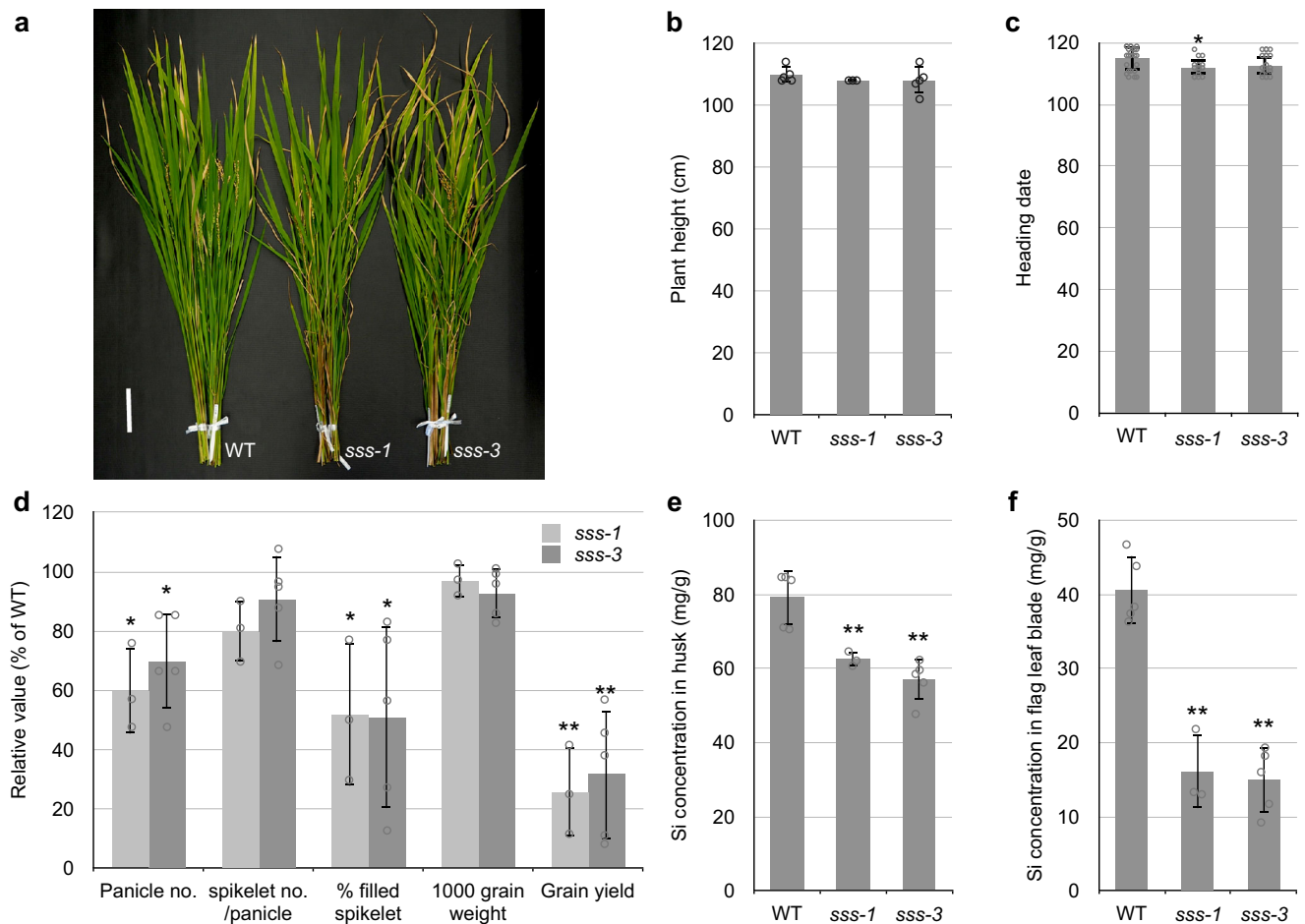


**Fig. 4 | Phenotype of *sss* mutants at the harvest.** WT and two independent *sss* knockout mutants were cultivated in soil pots and the phenotypes were compared at the harvest. **a** Appearance at the harvest. Bar = 10 cm. **b** Plant height. **c** Heading date. **d** Grain yield and yield factors relative to WT. **e, f** Si concentration in the husk

of filled grain (**e**) and flag leaf blade (**f**). Data represent mean  $\pm$  SD of 5 (WT, *sss-3*) or 3 (*sss-1*) (**b, d, e, f**) or 23 (WT), 21 (*sss-1*) or 25 (*sss-3*) (**c**) biological replicates. Significant differences compared with WT are marked with \* $p < 0.05$  or \*\* $p < 0.01$  by two-sided Tukey's test. Source data are provided as a Source Data file.

(Fig. 4d). Si concentration in the husk of filled grain and the flag leaf blade were decreased to 72–79% and 37–40% of the WT, respectively (Fig. 4e, f). On the other hand, concentrations of Mg in the husk and the flag leaf blade were increased in the mutants (Supplementary Figs. 11 and 12), probably due to the decreased grain yield/sink size (Fig. 4d).

### Shunting of the long-distance regulatory pathway in transgenic rice

To further demonstrate the regulatory function of SSS, we prepared transgenic rice carrying *Lsi1* promoter-*SSS::GFP*. This *Lsi1* promoter<sup>24</sup> results in ectopic high expression of *SSS::GFP* in root exodermis and endodermis, and possibly induces more expression of downstream target genes, including both endogenous *Lsi1*, *Lsi2*, and the own transgenic promoter. As a result, expressions of *Lsi1* and *Lsi2* were increased to 2 to 7 times higher than those of WT in the root of 5 independent transgenic lines (Fig. 5a, b). Root Si uptake was also enhanced up to 2 times of the WT (Fig. 5c). Although these gene expression levels and Si uptake were varied between 5 lines, the Si uptake showed a good positive correlation with the *SSS::GFP* expression level in the root ( $R^2 = 0.886$ ; Fig. 5d).

At the harvest of soil pot culture, WT and the transgenic lines showed no obvious differences, and 1000-grain weight, Si concentration in the husk and flag leaf blade were not different from WT (Supplementary Fig. 13). Therefore, the enhancement of Si uptake in the transgenic lines would be limited or saturated during the reproductive growth stage.

### Assessment of protein interaction between SSS and 14-3-3

Florigen (Hd3a in rice) makes ternary 'florigen activation complex' (FAC) together with 14-3-3 protein and a transcription factor OsFD1 in the shoot apical meristem and then FAC induces expression of downstream genes for flowering<sup>13,25</sup>. Therefore, we conducted a co-immunoprecipitation assay of SSS/OsFTL12 and GF14f (a major 14-3-3 protein in rice root) together with Hd3a as a positive control. When co-express Hd3a with GFP tag (Hd3a::GFP) and HA-tagged GF14f (HA::GF14f) in rice leaf protoplast, strong interaction between Hd3a and GF14f was observed (Supplementary Fig. 14). However, the interaction of SSS (SSS::GFP) with GF14f was much weaker than that of Hd3a, which is comparable to Hd3a<sub>F103A</sub> (mutation of a key residue for the interaction)<sup>25</sup> (Supplementary Fig. 14). SSS<sub>F98A</sub> mutation corresponding to Hd3a<sub>F103A</sub> (Supplementary Fig. 2) not largely affected the interaction with GF14f (Supplementary Fig. 14).

### Discussion

Based on the gene expression and response to Si (Fig. 1), phloem mobility and tissue localization of the protein (Figs. 1 and 2; Supplementary Fig. 6), the phenotypes of the knockout mutants and ectopic expression line (Figs. 3–5), SSS/OsFTL12 is hormonal signaling protein for adjustment of the root Si uptake. This function is distinct from any other florigen homologs identified so far. Rice and Arabidopsis have 19 and 6 homologs of FT in the genome, respectively (Supplementary Fig. 1). Among them, OsHd3a/AtFT (a major florigen), and some close homologs such as AtTSF and OsRFT1 were well characterized for the

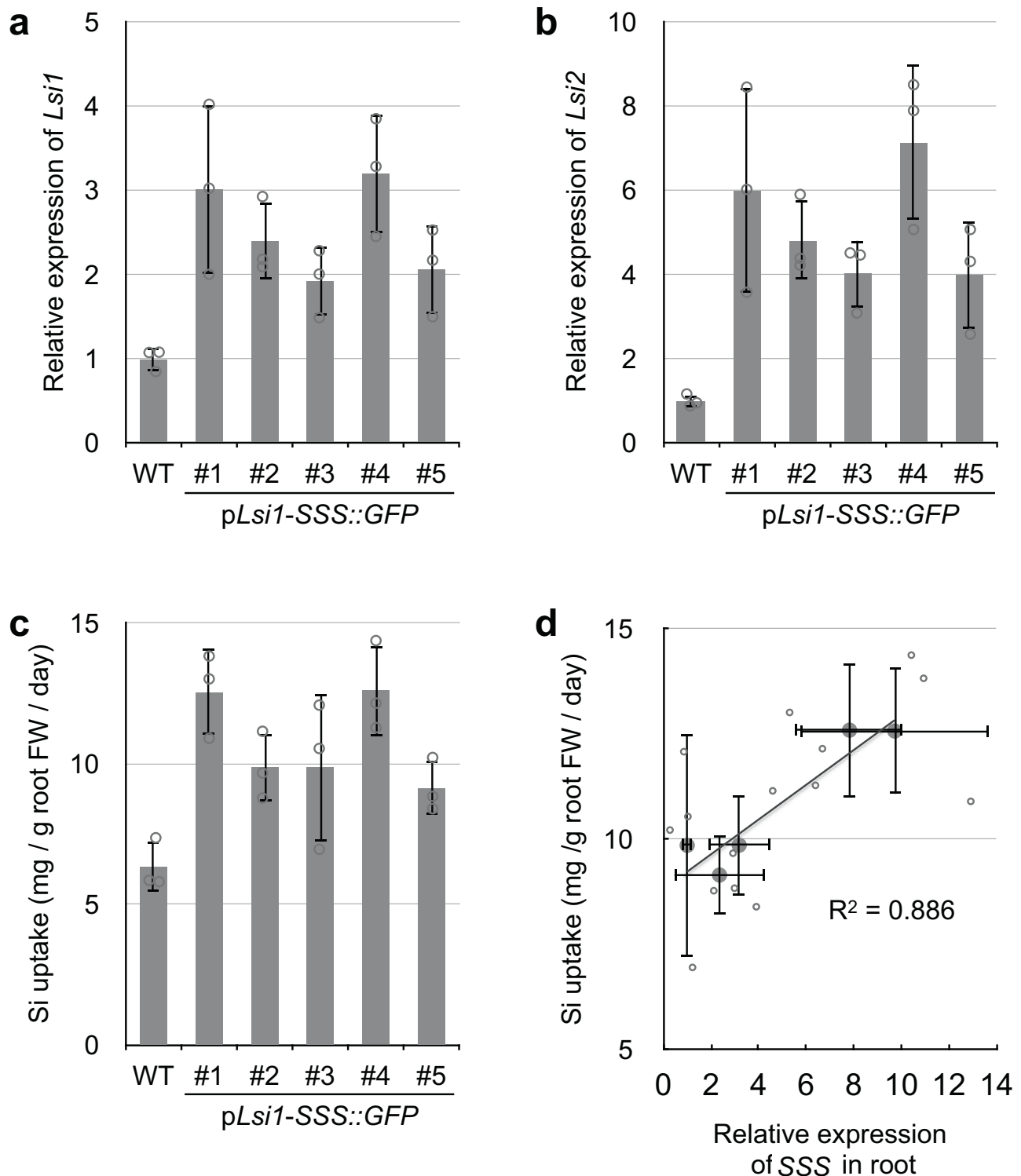


**Fig. 5 | Phenotype of *pLsi1-SSS::GFP* transgenic rice.** WT and 5 independent *pLsi1-SSS::GFP* transgenic rice lines were cultivated hydroponically without Si for 4 weeks. Then, each plant was used for (a, b) real-time RT-PCR gene expression analysis of *Lsi1* (a) *Lsi2* (b), and SSS (d) in the root, and 24 h Si (1 mM) uptake experiment (c).

The correlation between the *SSS::GFP* expression level in the root and the Si uptake is shown in (d). Data represent mean  $\pm$  SD of 3 biological replicates. Source data are provided as a Source Data file.

important role of the vegetative-to-reproductive phase transition<sup>13</sup>. Some other homologs, for example, *OrFTL9* in wild rice (*Oryza rufipogon*) involved in the regulation of grain size and number based on the maternal resources<sup>26</sup>, and *StSP6A* in potato (*Solanum tuberosum*) is involved in tuber induction<sup>27</sup>. Thus, all known florigen homologs (except SSS/*OsFTL12*) are cues for developmental regulation. From

this context, *OsFTL12* was recently also reported as a modulator of the heading date and plant architecture<sup>28</sup>. However, they did not pay attention to the Si, and almost all effects, including the heading date, were only observed in the over-expression transgenic rice but not in the *ftl12* knockout mutant<sup>28</sup>. They used a double 35S promoter to over-express *OsFTL12*<sup>28</sup>, which probably has higher expression, especially in

the meristematic tissues. In contrast, leaf- or node-derived SSS/OsFTL12 did not reach the shoot apical meristem (SAM) (Fig. 2c), different from florigen Hd3a<sup>13,29</sup>. They also demonstrated the interaction between OsFTL12 and a 14-3-3 protein GF14b<sup>28</sup>, similar to our result (Supplementary Fig. 14). Therefore, we think that ectopic expression of OsFTL12 within the SAM intercept 14-3-3 protein from the florigen activation complex (FAC) and act as florigen repression complex (FRC)<sup>28</sup>. Conversely, endogenous SSS/OsFTL12 directed to the root but not to the SAM (Figs. 1 and 2; Supplementary Fig. 6) has no role as either florigen or anti-florigen (Fig. 4c)<sup>28</sup>. Downstream target pathway(s) of SSS in root (Supplementary Table 2) and Hd3a in SAM should be different. Moreover, the interaction of SSS to 14-3-3 protein is much weaker than that of Hd3a and comparable to mutated Hd3a<sub>F103A</sub> (Supplementary Fig. 14), which almost impaired the FAC activity<sup>25</sup>. Thus, the intrinsic interaction partner(s) of SSS at the root probably differs from florigen.

SSS protein is phloem mobile (Fig. 1g) and reaches the root pericycle (Fig. 2e, l), but it is still away from exodermis and endodermis, which express major Si uptake transporters *Lsi1*<sup>5</sup> and *Lsi2*<sup>6</sup>. Although a faint signal of SSS::GFP was also observed in root endodermis (Fig. 2l), the symplastic connections between the endodermis and exodermis will be missing during the root aerenchyma development<sup>30</sup>. Therefore, *Lsi1* and *Lsi2* are probably not direct targets of SSS; more likely, some apoplastic diffusive molecule(s) relay the Si demand signal between them. Vice versa, the expression of SSS under the control of the *Lsi1* promoter can enhance root *Lsi1*, *Lsi2* expression, and the Si uptake (Fig. 5), but the gain is not as significant as expected by the short-cut positive feedback.

Transcriptome analysis (Supplementary Table 2) revealed that SSS protein attained to the root also regulates *Lsi3* and *OsNramp5* expression. *Lsi3* is a Si efflux transporter homologous to *Lsi2*/*SIET4*, and in the root, which is expressed in the pericycle and involved in Si uptake and xylem loading<sup>20</sup> together with *Lsi1* and *Lsi2*. *OsNramp5* is a dominant transporter for Mn and Cd root uptake localized in root exodermis and endodermis<sup>21</sup>, similar to *Lsi1* and *Lsi2*. Although *OsNramp5* expression was not a response to Mn, it was clearly down-regulated by Si accumulation<sup>23</sup>. Thus, SSS mediates all known Si responses of mineral transporters in rice roots, but the roles of most other genes potentially regulated by SSS in the root are unknown (Supplementary Table 2).

In the leaf, SSS is expressed in the phloem region of vascular tissues (Fig. 2). On the other hand, silicic acid taken up by the root transporters<sup>5,6</sup> is translocated through the xylem<sup>14,20,31</sup>, then unloaded from the leaf xylem by *Lsi6* (a homolog of *Lsi1*)<sup>32</sup>, finally transport out by *SIET4*<sup>4</sup> and deposit as amorphous silica on the leaf surface and in particular leaf epidermal cells (silica bodies and motor cells in rice)<sup>2,4,32</sup>. So, no contact has been found between the leaf/node phloem, which emanates the SSS signal, and the Si transport/deposition pathway. Moreover, no metabolite containing Si had been found in plants, and deposited silica is inert and much more stable compared to the life cycle of the grasses<sup>33</sup>, which means that very difficult to sense deposited silica by plants chemically. It is quite unclear how plants sense Si. But actually, a very sharp response of the SSS expression to Si was observed within a few hours after the root Si uptake (Fig. 1d). Surprisingly, now we found supersaturated silicic acid (more than 2 mM) in the phloem sap (Supplementary Fig. 5), although no any Si translocation pathway through the phloem had been reported as described above. Si concentrations in the phloem sap were nearly constant in each condition during several point samplings (5 to 32 h after Si supply) by the DIY-insect-laser method (Supplementary Fig. 5). It probably suggests that the phloem Si is not delivered through the phloem, but more likely provided the neighboring xylem. Therefore, rice plants can possibly sense the Si level in each part of the shoot phloem and then adjust the SSS expression independent of the silica deposition. It also suggests the presence of unknown mechanisms to prevent the

polymerization of supersaturated silicic acid within the phloem. Anyway, SSS is an invaluable clue to understanding the molecular mechanisms of plant Si sensing.

Si accumulation in plants has beneficial effects in alleviating various biotic and abiotic stresses<sup>2</sup>. Due to inert chemical properties and slow release of soluble Si in soil, it was considered that plants not over-accumulate Si and not suffer from excess toxicity of Si, but recently, a few exceptions at particular conditions have been reported. One is transgenic Arabidopsis carrying rice/wheat *Lsi1*, which results in leaf necrosis and growth defects depending on Si supply<sup>34</sup>. Because Arabidopsis (and probably Brassicaceae) exceptionally lacks the Si uptake transporter, *Lsi1* differs from most other species<sup>7</sup>, which probably also lacks mechanisms for proper Si deposition. Another one is the rice *siet4* mutant<sup>4</sup>. Because *SIET4* is a silicic acid efflux transporter involved in the final step of Si deposition in rice leaf, the mutant results in miscasting of Si in the leaf mesophyll tissues and induces unusual stress responses, which severely impair the growth<sup>4</sup>. Suggesting that accumulation and utilization of Si by plants postulate integrated mechanisms for the regulation, although these mechanisms are almost not manifested under the Si-rich environment on land. More benefits of Si are gained by the accumulation of Si, which appears to require more sophisticated regulatory mechanisms. Together with the preferential distribution control by inter-vascular transfer of Si in nodes<sup>14,15,31</sup>, dispatch of SSS from each Si shortage leaf and node, and transmission to the roots (Figs. 1 and 2; Supplementary Fig. 6) make it possible to integrate the demand of Si in the whole plant. The *sss* knockout mutants decreased the root Si uptake to half of the WT under Si insufficient conditions (Fig. 3).

The impact of Si uptake defect in *lsi1* mutant is much more obvious during the reproductive growth and, finally, decreases the grain yield 1/10 of the WT in field conditions<sup>9</sup>. Highest Si concentration was usually found in the husk (~10% of the dry weight). Rice (and graminaceous plants) developed a preferential Si distribution strategy to the husk by xylem to xylem inter-vascular transfer in the nodes<sup>14,15,31</sup>. Moreover, rice showed bimodal Si uptake and expression of *Lsi1* and *Lsi2*, temporally decreased after transplantation and rootage in the field; these are maximized around the heading<sup>9,35,36</sup>. This trend of Si uptake and distribution during reproductive growth corresponds to the SSS expression pattern in the field (Fig. 1a) and is consistent with higher expression and different responsibility to Si in the nodes (Fig. 1b, c). Si accumulation in the flag leaf and the grain yield of the *sss* mutants were decreased to about 1/3 of the WT in the soil culture condition with continuous Si supply (Fig. 4). Thus, healthy growth and productivity of rice presupposes the feedback modulation of Si accumulation by SSS even in the Si-rich environment.

Orthologs of SSS are conserved in graminaceous plants but not in the others (Supplementary Fig. 1). We demonstrated that the orthologs in wheat, maize and Moso bamboo also showed shoot-specific expression and response to Si similar to rice (Supplementary Fig. 3). SSS and the orthologs in cereal crops are possible can be used as indicators of the Si demand. Active uptake of Si by cereals often results in starvation of soluble Si in soil solution<sup>10,11</sup>. Therefore, the optimization of Si fertilization based on SSS levels has the potential to improve the productivity and sustainability of agriculture.

Poaceae is the latest plant family dominant on Earth's land surface and provides cereal crops for agriculture. It has evolved innovative traits different from other flowering plants, such as tillering growth and higher Si accumulation<sup>7,37</sup>. Grasses also developed the node-based nutrient distribution system, which enables grasses to more preferential Si deposition through the xylem to xylem inter-vascular transfer in nodes<sup>14,15,31</sup>. Now we realize that the innovation in graminaceous plants to utilize more Si to adapt to the environment on the Earth also requested the acquisition of a signaling protein SSS by neofunctionalization of a homolog of flowering hormone florigen. Si is a beneficial element but not an essential element for plants<sup>1</sup>. But now it is

clear that Si is deeply integrated into plants' strategy to adapt to land environments, especially in graminaceous plants. We need to consider a special niche of Si for plants, such as an "adaptive element".

## Methods

### Plant materials and growth conditions

The wild-type rice (WT, cv. Nipponbare), three independent knockout lines of SSS (*sss-1*, *sss-2*, and *sss-3*), and transgenic lines carrying fusion genes between SSS and GFP described below were used in this study. Seed germination and preparation of seedlings were as described previously using half-strength Kimura B nutrient solution or soil pot<sup>4</sup>. Seedlings of wheat (*Triticum aestivum* cv. Chinese spring), maize (*Zea mays* cv. B73), and Moso bamboo (*Phyllostachys edulis*) were prepared similarly but using 1/5 strength Hoagland solution with continuous aeration<sup>34</sup>. The plants were grown in a controlled greenhouse under natural light at 25 to 30 °C for rice, maize, and Moso bamboo or at 20 to 25 °C for wheat. All experiments were performed with at least three biological replicates.

### Generation of knockout lines of SSS by CRISPR/Cas9

We generated knockout lines of SSS using the CRISPR/Cas9 technique. Two different target sequences for *sss-1* and *sss-2/3* at the first exon of SSS were selected. The primers are listed in Supplementary Table 3. The single guide RNA vector (pU6gRNA) and plant expression vector of Cas9 (pZDgRNA\_Cas9ver.2\_HPT) were used as described before<sup>38</sup>. The derived constructs were transformed into rice (cv. Nipponbare) calluses according to Hiei et al.<sup>39</sup>. Three independent homologous knockout lines, *sss-1*, -2, -3 were selected for further analysis.

### Preparation of SSS-GFP fusion gene and generation of transgenic rice

The ORFs of SSS (Os06g0552900) and GFP without stop codon were amplified by PCR (Supplementary Table 3) and were inserted into CaMV 35S-GFP vector<sup>40</sup>, resulting in *SSS::GFP* and *SSS::GFPGFP*. These plasmids were used for transient expression in onion epidermis cells by particle bombardment<sup>40</sup>. Two kb upstream and 1.7 kb downstream sequences of SSS were also cloned separately (Supplementary Table 3) and inserted into the pPZP2H-lac binary vector<sup>41</sup> together with *SSS::GFP* or *SSS::GFPGFP*. To prepare the over-expression to construct in the root, *SSS::GFP* was inserted between the *LsiI* promoter and *NOS* terminator in pPZP2H-lac binary vector<sup>42</sup>. The derived constructs were transformed into rice (cv. Nipponbare) calluses, according to Hiei et al.<sup>39</sup>.

### Gene expression analysis of SSS

To investigate the SSS spatial and temporal expression pattern in paddy field conditions, we used the cDNA of different organs as indicated in Fig. 1a, which was prepared in a previous study<sup>16</sup>. To investigate the Si response of SSS, *LsiI*, and *Lsi2* in rice, and the SSS orthologs in wheat, maize, and Moso bamboo at the vegetative growth stage, 3 to 5-leaf stage seedlings pre-cultured hydroponically without Si were used for Si treatment as indicated in figure legends. The total RNA of each organ was extracted using an RNeasy plant mini kit (QIAGEN) followed by cDNA synthesis according to the manufacturer of Revert-Ace (TOYOBO). Specific cDNAs were amplified by SsoFast Eva-Green Supermix (Bio-Rad), and quantitative real-time PCR was performed on CFX Opus 384 (Bio-Rad). *HistoneH3*, *Actin*,  $\alpha$ -*tubulin*, or *Ubiquitin* were used as internal controls. The primers used are listed in Supplementary Table 3. The relative expression was normalized based on internal control genes by  $\Delta\Delta Ct$  method using the CFX Maestro software (Bio-Rad).

### Immunostaining of SSS::GFP

To observe the tissue-specific localization and subcellular localization of SSS, we performed immunostaining in transgenic rice carrying pSSS-*SSS::GFP* or pSSS-*SSS::GFPGFP* with an antibody against GFP (A11122,

Invitrogen) as described previously<sup>35</sup>. For observation of subcellular localization, 4',6-diamidino-2-phenylindole (DAPI) for nucleic acid staining was used. The fluorescence signal was observed by confocal laser scanning microscopy (TCS SP8x, Leica Microsystems).

### Si uptake experiment and determination of Si concentration

Four-week-old WT rice, three *sss* knockout mutants, and 5 independent *pLsiI-SSS::GFP* transgenic lines pre-cultured hydroponically without Si were put in a half-strength Kimura B solution containing 1 mM silicic acid. Three hours (for mutants) or 24 h (for transgenic lines) after, a part of the uptake solution was collected for determination of the Si concentration remaining in the uptake solution as described previously<sup>20</sup>. Water loss was also recorded. Then, the roots and shoots were harvested separately, and their fresh weights were recorded. The Si concentration in the uptake solution was determined by the colorimetric molybdenum blue method<sup>43</sup>.

### Phenotypic analysis of *sss* mutants in soil culture

For soil culture, seedlings (16-day-old) of WT, two *sss* mutants, and *pLsiI-SSS::GFP* transgenic lines pre-cultured hydroponically were transplanted to a 1/5000 a Wagner pot containing 3.5 kg soil collected from the experimental field at Okayama University, amended with 50 g of Water Silica (Fuji Silysia Chemical). Plants were watered daily and grown until maturation. At harvest, plant height and yield components (panicle number per plant, spikelet number per panicle, filled spikelet rate, 1000-grain weight) were measured, and grain yields per plant were calculated. For determination of Si, husk and flag leaf blades dried at 70 °C were digested in a microwave oven (Microwave Digestion System START D, Millstone Co., Ltd.) as described previously<sup>4</sup>. The Si concentration in the digested solution was determined by the colorimetric molybdenum blue method as described above. The other mineral concentrations were determined by ICP-MS (7700X; Agilent Technologies).

### Acquisition of phloem sap by DIY-insect-laser method

Eight leaf stage seedlings of WT, *sss-1*, and *LsiI* mutants pre-treated with or without 1 mM Si for the last 3 days were transplanted to 500 mL plastic pot with nutrient solution containing 1 or 0.1 mM Si and detached the lower 1–4 leaves. Each plant was covered by an acrylic resin tube with a 46 mm inner diameter and put in a few adult brown planthoppers (*Nilaparvata lugens*), then incubated in a room at 28–30 °C and 60% RH. After starting sucking, the stylet of the insect was aimed and cut by a commercial laser engraver LaserPecker 2 (LaserPecker). Spill-out sap from the stylet cut end was collected by a glass capillary (Microcap 2  $\mu$ L, Drummond Scientific). Obtained phloem saps were applied for Si determination by ICP-MS (8900; Agilent Technologies), western blot as described below, and proteome analysis service in Okayama University ([http://www.okayama-u.ac.jp/user/grcweb/dgpweb/GRC\\_home-J.html](http://www.okayama-u.ac.jp/user/grcweb/dgpweb/GRC_home-J.html)). A brief method of the proteome analysis is below. Protein samples in phloem saps (1.2–2.0  $\mu$ L) were purified by chloroform/methanol precipitation, alkylated in 200 mM iodoacetamide and 25 mM ammonium bicarbonate for 1 h at room temperature, and digested by trypsin (Promega) for 24 h at 37 °C. Then, the samples were applied for LC-MS/MS (amazon ETD-OF/nanoElute; Bruker Japan, Yokohama, Japan) and analyzed by MascotServer version 2.8.2 (Matrix Science, UK).

### Preparation of recombinant SSS protein

The open reading frame of SSS gene was cloned into the pMal-p5X vector (NEW ENGLAND Biolabs) and expressed with an N-terminal tobacco etch virus (TEV) protease-cleavable MBP tag and octa-His affinity tag in *Escherichia coli* C43(DE3) cells (Lucigen). LB medium (1 liter) containing 100  $\mu$ g/mL ampicillin was inoculated with 20 mL of an overnight C43 culture. Cells were grown at 37 °C with shaking until the absorbance at 600 nm reached 0.6, induced with 0.5 mM isopropyl 1-

thio- $\beta$ -D-galactopyranoside, and grown for another 21 h at 30 °C with shaking. Cells were harvested by centrifugation at 8000  $\times g$  for 10 min at 4 °C, and washed with phosphate-buffered saline (PBS). The cell pellet was resuspended in lysis buffer (50 mM Tris-HCl, pH 8.0, 500 mM NaCl, 1.5  $\mu$ M aprotinin, 10  $\mu$ M leupeptin, 10  $\mu$ g/mL trypsin inhibitor, 3.75  $\mu$ g/mL DNase I, 1 mM phenylmethylsulfonyl fluoride (PMSF), and 0.5  $\mu$ g/mL lysozyme), incubated for 10 min at room temperature with shaking and disrupted by sonication on ice. The cell debris was removed by ultracentrifugation at 104,200  $\times g$  for 30 min at 4 °C. The supernatant was incubated with amylose resin (NEW ENGLAND Biolabs) for 2 h at 4 °C. The resin was loaded onto an open column, washed with wash buffer (20 mM Tris-HCl, pH 8.0, 500 mM NaCl), and incubated with hexa-His-tagged TEV<sub>SH</sub><sup>44</sup> (10:1 mass ratio of SSS to TEV<sub>SH</sub>) for overnight. The resin was loaded onto an open column, and eluting SSS was collected by gravity flow. The flow-through was loaded onto a Superdex 75 Increase 10/300 GL size-exclusion column equilibrated with PBS. Peak fractions were pooled and used for western blotting analysis.

### Western blot analysis of SSS, SSS::GFP, and SSS::GFP:GFP protein

The synthetic peptide C-QRPTGTGRRPT (positions 162–173 of SSS) was used to immunize rabbits to obtain antibodies against SSS. The obtained antiserum was purified through a peptide affinity column before use. For GFP fusion proteins, anti-GFP (B-2 mouse IgG monoclonal, SC-9996, Santa Cruz Biotechnology) was used. Crude protein was extracted both from the root and shoot grown in different Si conditions (-Si and +1 mM Si for 10 h, 24 h, 72 h). Shoot or root samples were ground in powder with liquid nitrogen and suspended in the extraction buffer containing 150 mM NaCl, 50 mM Tris-HCl (pH 7.5), 0.1% Tween 20, 10% glycerol, 1 mM DTT, and protease inhibitor cocktail (Sigma). After 30 min incubation on ice, the extracts were centrifuged at 13,000 rpm 4 °C for 20 min. The supernatant was separated by SDS-PAGE and subjected to immunoblotting using the anti-SSS antibody. After washing with TBS-T, the membranes were incubated with anti-rabbit IgG conjugated to HRP (W401B, Promega) or anti-mouse IgG conjugated to HRP (W402B, Promega). Phloem sap was collected by insect-laser method from WT and *sss-1* mutant with or without Si for 3 days as described above. 0.18 to 0.32  $\mu$ L of phloem sap and 0.5  $\mu$ L of xylem sap<sup>4</sup> were used for the detection of SSS protein. 10 ng of recombinant SSS protein was used as a control. Both phloem and xylem sap were mixed with 6 $\times$ SDS-PAGE sample buffer and separated by the SDS-PAGE and followed by immunoblotting described above.

### Recovery of SSS expression by Si starvation

Three-week-old seedlings pre-treated with or without 1 mM Si for 7 days were subjected to Si starvation treatment for another 7 days. Time-dependent gene expression in the shoot and protein abundance in the root were determined by real-time RT-PCR and western blot, respectively. Recovery of gene expression and protein abundance in different tissues (root, mature leaf blade, and newly expanded leaf blade) were also investigated.

### Protein interaction assay between SSS and 14-3-3

The ORFs of *Hd3a* (Os06g0157700) and *GF14f* (Os03g0710800) with N-terminal HA-tag were amplified by PCR (Supplementary Table 3). Point mutation of *Hd3a*<sub>F103A</sub> and *SSS*<sub>F98A</sub> were introduced by PCR (Supplementary Table 3). Replace SSS or SSS::GFP of CaMV 35S-SSS::GFP plasmid described above by the PCR products, *Hd3a*, *HA-GF14f*, *Hd3a*<sub>F103A</sub>, or *SSS*<sub>F98A</sub>. The protoplasts were isolated based on the methods reported by Zhang et al.<sup>45</sup> with slight modifications. 200  $\mu$ L of protoplasts were mixed with 4  $\mu$ g plasmid of *GFP*, *Hd3a*::*GFP*, *Hd3a*<sub>F103A</sub>::*GFP*, *SSS*::*GFP*, *SSS*<sub>F98A</sub>::*GFP* and 2  $\mu$ g of plasmids for *HA-GF14f*, and 220  $\mu$ L of PEG solution (40% PEG 4000, 0.3 M mannitol and 0.1 M CaCl<sub>2</sub>). The transformation mixture was incubated for 15 min in

darkness at 25 °C. The mixture was collected by centrifugation, resuspended in 1 mL WI solution (4 mM MES, pH 5.7, 0.5 M mannitol, and 20 mM KCl), and incubated for 14 h at 25 °C. The protoplasts were harvested by centrifugation and homogenized in IP buffer (50 mM Tris-HCl, pH 8.0, 100 mM sodium phosphate buffer, 40 mM NaCl, 1% Triton X-100, 0.5 mM EDTA, 1 mM PMSF, and 1% protease inhibitor) with sonication, then centrifuged. 3  $\mu$ L of GFP trap magnetic agarose (B-2 mouse IgG monoclonal, SC-9996, Santa Cruz Biotechnology) were added to the supernatant, and incubated for 4 h at 4 °C with gentle shaking. After being washed by wash buffer (10 mM Tris-HCl pH 8 and 500 mM NaCl, 500 mM EDTA, and 0.1% Triton X-100), the proteins were eluted from the beads by boiling in SDS-PAGE sample buffer for 5 min and analyzed by western blotting. The HRP conjugate anti-mouse IgG (W402B, LOT0000523668, Promega) and anti-HA (3F10, 12013819001, Roche) antibodies were used.

### Phylogenetic analysis

Amino acid sequences of SSS/FTL12 homologs in rice, Arabidopsis and some other species (as shown in Supplemental Fig. 1), were acquired from the database by BLAST search (<https://blast.ncbi.nlm.nih.gov/>). Sequence alignment by ClustalW and phylogenetic analysis by Maximum Likelihood method with 1000 bootstraps were conducted using MEGA X<sup>46</sup>.

### Statistics and reproducibility

Statistical analyses were performed by two-sided Tukey's-test using the software BellCurve for Excel (Social Survey Research Information Co. Ltd, Tokyo, Japan). All experiments were repeated at least two times, and similar results were obtained.

### Transcriptome analysis of WT and *sss* root

Transcriptome analysis was performed similarly to the previous study<sup>4</sup>. Seedlings (21-day-old) cultured in solution free of Si were treated with or without 1 mM Si for 2 days. Total RNA was extracted from the whole root of both WT and *sss-1* mutants using an RNeasy Plant Mini Kit (Qiagen). RNA-seq was performed using a DNBSEQ-G400FAST (MGI, Kobe, Japan) for paired-end sequencing. A total of 30 million to 40 million stranded paired-end (2 $\times$ 150 bp) sequences were obtained for each sample. Three biological replicates were made for each line and treatment. Sequences were mapped on IRGSP-1.0 rice reference genome (<https://rapdb.dna.affrc.go.jp>), and the FPKM (fragments per kilobase of exon per million mapped reads) values were compared using TopHat and Cufflinks on Galaxy/NAAC server (<https://galaxy.dna.affrc.go.jp>). Genes with a significant difference (>2-fold, <0.05 False Discovery Rate, FPKM > 10 in either WT -Si or *sss* -Si) in expression between the *sss* mutant and WT without Si were extracted. The genes up- and downregulated in the mutant were further used for gene ontology (GO) enrichment analysis, which was performed using PANTHER19.0 (<http://pantherdb.org>).

### Reporting summary

Further information on research design is available in the Nature Portfolio Reporting Summary linked to this article.

### Data availability

The experiment data that support the findings of this study are available from the corresponding author upon request. The RNA-seq data generated in this study have been deposited to DDBJ BioProject under accession number PRJDB18916. The source data for Figs. 1, 3 to 5 and Supplementary Figs. 3 to 5, 11 to 13 are provided as a Source Data file. Source data are provided in this paper.

### References

1. Rengel, Z. Cakmak, I. & White, P. J. (eds). *Marschner's Mineral Nutrition of Plants*. 4th edn. (Academic Press, 2023).

2. Ma, J. F. & Yamaji, N. Silicon uptake and accumulation in higher plants. *Trends Plant Sci.* **11**, 392–397 (2006).
3. Ranjan, A. et al. Silicon-mediated abiotic and biotic stress mitigation in plants: underlying mechanisms and potential for stress resilient agriculture. *Plant Physiol. Biochem.* **163**, 15–25 (2021).
4. Mitani-Ueno, N. et al. A silicon transporter gene required for healthy growth of rice on land. *Nat. Commun.* **14**, 6522 (2023).
5. Ma, J. F. et al. A silicon transporter in rice. *Nature* **440**, 688–691 (2006).
6. Ma, J. F. et al. An efflux transporter of silicon in rice. *Nature* **448**, 209–212 (2007).
7. Ma, J. F. & Yamaji, N. A cooperative system of silicon transport in plants. *Trends Plant Sci.* **20**, 435–442 (2015).
8. Hodson, M. J., White, P. J. & Broadley, M. R. Phylogenetic variation in the silicon composition of plants. *Ann. Bot.* **96**, 1027–1046 (2005).
9. Tamai, K. & Ma, J. F. Reexamination of silicon effects on rice growth and production under field conditions using a low silicon mutant. *Plant Soil* **307**, 21–27 (2008).
10. Struyf, E. et al. Historical land use change has lowered terrestrial silica mobilization. *Nat. Commun.* **1**, 129 (2010).
11. Ma, J. F. & Takahashi, E. *Soil, Fertilizer, and Plant Silicon Research in Japan* (Elsevier, 2002).
12. Mitani-Ueno, N., Yamaji, N. & Ma, J. F. High silicon accumulation in the shoot is required for down-regulating the expression of Si transporter genes in rice. *Plant Cell Physiol.* **57**, 2510–2518 (2016).
13. Tsuji, H. & Sato, M. The function of florigen in the vegetative-to-reproductive phase transition in and around the shoot apical meristem. *Plant Cell Physiol.* **65**, 322–337 (2024).
14. Yamaji, N., Sakurai, G., Mitani-Ueno, N. & Ma, J. F. Orchestration of three transporters and distinct vascular structures in node for intervascular transfer of silicon in rice. *Proc. Natl Acad. Sci. USA* **112**, 11401–11406 (2015).
15. Yamaji, N. & Ma, J. F. Node-controlled allocation of mineral elements in Poaceae. *Curr. Opin. Plant Biol.* **39**, 18–24 (2017).
16. Yamaji, N. et al. Reducing phosphorus accumulation in rice grains with an impaired transporter in the node. *Nature* **541**, 92–95 (2017).
17. Kawabe, S., Fukumorita, T. & Chino, M. Collection of rice phloem sap from stylets of homopterous insects severed by YAG laser. *Plant Cell Physiol.* **21**, 1319–1327 (1980).
18. Aki, T., Shigyo, M., Nakano, R., Yoneyama, T. & Yanagisawa, S. Nano scale proteomics revealed the presence of regulatory proteins including three FT-like proteins in phloem and xylem saps from rice. *Plant Cell Physiol.* **49**, 767–790 (2008).
19. Miras, M. et al. Plasmodesmata and their role in assimilate translocation. *J. Plant Physiol.* **270**, 153633 (2022).
20. Huang, S. et al. A pericycle-localized silicon transporter for efficient xylem loading in rice. *N. Phytol.* **234**, 197–208 (2022).
21. Sasaki, A., Yamaji, N., Yokosho, K. & Ma, J. F. Nramp5 is a major transporter responsible for manganese and cadmium uptake in rice. *Plant Cell* **24**, 2155–2167 (2012).
22. Huang, X. Y. et al. Natural variation in a molybdate transporter controls grain molybdenum concentration in rice. *N. Phytol.* **211**, 1983–1997 (2019).
23. Shao, J. F., Che, J., Yamaji, N., Shen, R. F. & Ma, J. F. Silicon reduces cadmium accumulation by suppressing expression of transporter genes involved in cadmium uptake and translocation in rice. *J. Exp. Bot.* **68**, 5641–5651 (2017).
24. Konishi, N., Mitani-Ueno, N., Yamaji, N. & Ma, J. F. Polar localization of a rice silicon transporter requires isoleucine at both C- and N-termini as well as positively charged residues. *Plant Cell* **35**, 2232–2250 (2023).
25. Taoka, K. et al. 14-3-3 proteins act as intracellular receptors for rice Hd3a florigen. *Nature* **476**, 332–335 (2011).
26. Ta, K. N. et al. A leaf-emanated signal orchestrates grain size and number in response to maternal resources. *Plant J.* **115**, 175–189 (2023).
27. Teo, C. J., Takahashi, K., Shimizu, K., Shimamoto, K. & Taoka, K. Potato tuber induction is regulated by interactions between components of a tuberigen complex. *Plant Cell Physiol.* **58**, 365–374 (2017).
28. Zheng, R. et al. OsFTL12, a member of FT-like family, modulates the heading date and plant architecture by florigen repression complex in rice. *Plant Biotech. J.* **21**, 1343–1360 (2023).
29. Tamaki, S. et al. FT-like proteins induce transposon silencing in the shoot apex during floral induction in rice. *Proc. Natl Acad. Sci. USA* **112**, E901–E910 (2015).
30. Yamauchi, T., Shimamura, S., Nakazono, M. & Mochizuki, T. Aerenchyma formation in crop species: a review. *Field Crops Res.* **152**, 8–16 (2013).
31. Yamaji, N. & Ma, J. F. A transporter at the node responsible for intervascular transfer of silicon in rice. *Plant Cell* **21**, 2878–2883 (2009).
32. Yamaji, N., Mitani, N. & Ma, J. F. A transporter regulating silicon distribution in rice shoots. *Plant Cell* **20**, 1381–1389 (2008).
33. International Committee for Phytolith Taxonomy (ICPT). International Code for Phytolith Nomenclature (ICPN) 2.0. *Ann. Bot.* **124**, 189–199 (2019).
34. Montpetit, J. et al. Cloning, functional characterization and heterologous expression of TaLsi1, a wheat silicon transporter gene. *Plant Mol. Biol.* **79**, 35–46 (2012).
35. Yamaji, N. & Ma, J. F. Spatial distribution and temporal variation of the rice silicon transporter Lsi1. *Plant Physiol.* **143**, 1306–1313 (2007).
36. Yamaji, N. & Ma, J. F. Further characterization of a rice silicon efflux transporter, Lsi2. *Soil Sci. Plant Nutr.* **57**, 259–264 (2011).
37. Strömberg, C. A. Evolution of grasses and grassland ecosystems. *Annu. Rev. Earth Planet. Sci.* **39**, 517–544 (2011).
38. Che, J., Yokosho, K., Yamaji, N. & Ma, J. F. A vacuolar phytosiderophore transporter alters iron and zinc accumulation in polished rice grains. *Plant Physiol.* **181**, 276–288 (2019).
39. Hiei, Y., Ohta, S., Komari, T. & Kumashiro, T. Efficient transformation of rice (*Oryza sativa* L.) mediated by *Agrobacterium* and sequence analysis of the boundaries of the T-DNA. *Plant J.* **6**, 271–282 (1994).
40. Yamaji, N., Sasaki, A., Xia, J. X., Yokosho, K. & Ma, J. F. A node-based switch for preferential distribution of manganese in rice. *Nat. Commun.* **4**, 2442 (2013).
41. Fuse, T., Sasaki, T. & Yano, M. Ti-plasmid vectors useful for functional analysis of rice genes. *Plant Biotechnol.* **18**, 219–222 (2001).
42. Huang, S. et al. Boron uptake in rice is regulated post-translationally via a clathrin-independent pathway. *Plant Physiol.* **188**, 1649–1664 (2022).
43. Ma, J. F., Higashitani, A., Sato, K. & Takeda, K. Genotypic variation in silicon concentration of barley grain. *Plant Soil* **249**, 383–387 (2003).
44. van den Berg, S., Lofdahl, P. A., Hard, T. & Berglund, H. Improved solubility of TEV protease by directed evolution. *J. Biotechnol.* **121**, 291–298 (2006).
45. Zhang, Y. et al. A highly efficient rice green tissue protoplast system for transient gene expression and studying light/chloroplast-related processes. *Plant Method.* **7**, 30 (2011).
46. Stecher, G., Tamura, K. & Kumar, S. Molecular evolutionary genetics analysis (MEGA) for macOS. *Mol. Biol. Evol.* **37**, 1237–1239 (2020).

## Acknowledgements

This work was supported by the Japan Society for the Promotion of Science (JSPS) (KAKENHI grant no. 21H05034 to JFM, 19H03250, 24H00571 to NY, 24K08648 to NM-U), Takeda Science Foundation to NY, and Ohara Syonokai Foundation to NY and TS. We thank Prof. Ivan Galis for providing a brown planthopper. We also thank Dr. Masaki Endo for providing pU6gRNA and pZDgRNA\_Cas9ver.2\_HPT for the generation of CRISPR/Cas9 lines.

## Author contributions

N.Y. and N.M.-U. designed the experiments and analyzed the data. N.M.-U., N.Y., T.F., T.S., J.F.S., S.W., and Y.S. performed the experiments. N.Y., N.M.-U., and J.F.M. wrote the article. All authors discussed the results and read the manuscript.

## Competing interests

The authors declare no competing interests.

## Additional information

**Supplementary information** The online version contains supplementary material available at <https://doi.org/10.1038/s41467-024-55322-7>.

**Correspondence** and requests for materials should be addressed to Naoki Yamaji.

**Peer review information** *Nature Communications* thanks Dai-Yin Chao, Mutsutomo Tokizawa and the other, anonymous, reviewer for their contribution to the peer review of this work. A peer review file is available.

**Reprints and permissions information** is available at <http://www.nature.com/reprints>

**Publisher's note** Springer Nature remains neutral with regard to jurisdictional claims in published maps and institutional affiliations.

**Open Access** This article is licensed under a Creative Commons Attribution-NonCommercial-NoDerivatives 4.0 International License, which permits any non-commercial use, sharing, distribution and reproduction in any medium or format, as long as you give appropriate credit to the original author(s) and the source, provide a link to the Creative Commons licence, and indicate if you modified the licensed material. You do not have permission under this licence to share adapted material derived from this article or parts of it. The images or other third party material in this article are included in the article's Creative Commons licence, unless indicated otherwise in a credit line to the material. If material is not included in the article's Creative Commons licence and your intended use is not permitted by statutory regulation or exceeds the permitted use, you will need to obtain permission directly from the copyright holder. To view a copy of this licence, visit <http://creativecommons.org/licenses/by-nc-nd/4.0/>.

© The Author(s) 2024